Identification and Characterization of a FcR Homolog in an Ectothermic Vertebrate, the Channel Catfish (*Ictalurus punctatus*)[1,2]

James L. Stafford,* Melanie Wilson,* Deepak Nayak,* Sylvie M. Quiniou,[†] L. W. Clem,* Norman W. Miller,* and Eva Bengtén[3]*

An FcR homolog (IpFcRI), representing the first such receptor from an ectothermic vertebrate, has been identified in the channel catfish (*Ictalurus punctatus*). Mining of the catfish expressed sequence tag databases using mammalian FcR sequences for CD16, CD32, and CD64 resulted in the identification of a teleost Ig-binding receptor. IpFcRI is encoded by a single-copy gene containing three Ig C2-like domains, but lacking a transmembrane segment and cytoplasmic tail. The encoded Ig domains of IpFcRI are phylogenetically and structurally related to mammalian FcR and the presence of a putative Fc-binding region appears to be conserved. IpFcRI-related genomic sequences are also present in both pufferfish and rainbow trout, indicating the likely presence of a soluble FcR in other fish species. Northern blot and qualitative PCR analyses demonstrated that IpFcRI is primarily expressed in IgM-negative leukocytes derived from the lymphoid kidney tissues and PBL. Significantly lower levels of IpFcRI expression were detected in catfish clonal leukocyte cell lines. Using the native leader, IpFcRI was secreted when transfected into insect cells and importantly the native IpFcRI glycoprotein was detected in catfish plasma using a polyclonal Ab. Recombinant IpFcRI binds catfish IgM as assessed by both coimmunoprecipation and cell transfection studies and it is presumed that it functions as a secreted FcR akin to the soluble FcR found in mammals. The identification of an FcR homolog in an ectothermic vertebrate is an important first step toward understanding the evolutionary history and functional importance of vertebrate Ig-binding receptors. *The Journal of Immunology*, 2006, 177: 2505–2517.

R eceptors specific for the Fc portion of Ig (i.e., FcR) are expressed by a wide variety of mammalian cells of hemopoietic origin. In general, FcR participate in activation or inhibition of immune responses following the recognition of monomeric Ig or Ig in the form of immune complexes. Since early reports describing the presence of FcR on macrophages (1) and lymphocytes (2–4), more recent studies have expanded the understanding of the genomics and functional significance of these important innate immune receptors.

In humans, eight genes found on chromosome 1q21-23 encode for the IgG FcR family (FcγR) (5–7). These include the high-affinity FcγRI (*RIA*, *RIB*, and *RIC*) as well as the low-affinity FcγRII (*RIIA*, *RIIB*, and *RIIC*) and FcγRIII (*RIIIA* and *RIIIB*). Comparatively, only three genes, split between two different chromosomes, encode for the mouse FcγR (5, 8). Recently, a murine IgG FcR (FcγRIV) with preferential specificity for IgG2a and

IgG2b has been described, and it appears to be conserved in all mammalian species (9). Receptors for IgE (FcεR) are present in both humans and mice (10, 11), and a novel FcR that binds to both IgM and IgA isotypes (Fcα/μR) has also been reported in mammals (12, 13).

In most instances, the classical mammalian FcR genes encode for immune receptors consisting of extracellular C2 Ig domains (D),[4] a transmembrane (TM) segment, and a cytoplasmic tail (CYT) that may contain signaling motifs. The membrane distal D1 and D2 Ig domains of FcγRI are structurally related to the two Ig domains of the low-affinity receptors, albeit the acquisition of a third membrane proximal domain (D3) is necessary for the high-affinity Ig binding exhibited by FcγRI (14–17). Depending on the type of FcR engaged, cellular activation or inhibition occurs through association with adaptor molecules or signaling motifs present within the CYT. In addition to the positive and negative regulation of cellular responses, FcR also participate in the uptake and clearing of immune complexes as well as the transport of Ig (18).

Alternative splicing and proteolytic cleavage of membrane-associated FcR have been shown to generate soluble forms of these receptors (sFcR) (19). For example, alternative splicing results in the generation of a TM-deleted FcγRIIb2 mRNA (termed FcγRIIb3), providing a third isoform encoded by the single murine *FcγRII* gene (8, 20). This FcγRIIb3 is a secreted protein and has been identified in culture supernatants of macrophage cell lines

expressing FcγRIIb2 (20). A similar mechanism also has been identified in humans for the *FcγRIIa* gene, which is secreted by Langerhans cells and K562 and U937 cell lines (21). In activated neutrophils and macrophages, proteolytic cleavage of the membrane bound FcγRIII releases sFcγRIII, which represents the major form of sFcR found in human plasma (22, 23). Although the biological significances of sFcR are not entirely understood, mammalian sFcR can inhibit the binding of immune complexes to FcγR-positive cells, down-regulate B cell proliferation and Ab production, and trigger cellular activation by binding to complement receptors (19, 21, 24–26).

To date, Ig-binding FcR homologs have not been identified in any ectothermic vertebrate, although it is well established that these animals produce Abs (reviewed in Ref. 27). Several studies suggest that immune cells in amphibians, fish, and sharks bind to Ig, presumably through Fc-like receptors (28–37), and it is speculated that the transfer of Abs from mother to eggs in teleosts and elasmobranches is also a FcR-mediated process (38, 39). However, despite this functional evidence, an Ig-binding FcR homolog in these animals has not been identified, which has limited the understanding of not only the evolutionary history of Ig-binding receptors but also their functional significance in ectotherms. In this study, we report the initial identification and preliminary functional characterization of a novel Ig-binding soluble FcR homolog from the channel catfish.

Materials and Methods

Experimental animals, cell lines, and mAbs

Catfish (1–2 kg) were maintained in individual tanks as described previously (40). The 1G8 and 3B11 lines are cloned autonomous B cells generated from two different out bred catfish by mitogen stimulation (41, 42). The 42TA is a macrophage cell line (42), and TS32.17 is a cloned nonautonomous Ag-dependent cytotoxic T cell line, which requires weekly stimulation with irradiated allogeneic cells for continuous proliferation (43). An MLC was developed by in vitro stimulation of naive catfish PBL with irradiated 3B11 cells and maintained by weekly stimulation (44). Catfish cell lines were grown at 27°C in a modified mixture of AIM-V and L-15 (Invitrogen Life Technologies) supplemented with 3% normal catfish serum (CFS) as described previously (42). The HeLa cell line was obtained from American Type Culture Collection and grown in DMEM (Sigma-Aldrich) with 10% FBS.

Mouse mAbs 9E1 (IgG1, κ) and 1H12 (IgG1, κ) react with catfish IgM H chain (45); mAb 9E1 was used for flow cytometry and 1H12 for Western blot analyses. mAb 1.14 is an isotype control that reacts with rainbow trout (*Oncorhynchus mykiss*) IgM H chain, but not with catfish IgM (46). Hybridoma cells were grown at 37°C in DMEM supplemented with 10% FBS. Hybridoma culture supernatants were used directly as the mAb source and contained equivalent IgG concentrations as determined by ELISA and Western blot analyses.

Fractionation of catfish leukocytes

Leukocyte isolation and fractionation were performed using a combination of Percoll gradients (Sigma-Aldrich) and MACS. Briefly, catfish leukocytes were isolated from heparinized blood and homogenized tissues (spleen, pronephros, and mesonephros) by centrifugation on a cushion of Ficoll-Hypaque (Lymphoprep; Accurate Chemical) (42). Leukocytes (2×10^8) were separated into IgM-negative and IgM-positive fractions using mAb 9E1 and MiniMACs separation columns (Miltenyi Biotec) according to the manufacturer's protocol. The IgM-negative fraction was resuspended in 3 ml of RPMI 1640 medium and layered onto a discontinuous 34% and 51% Percoll gradient and centrifuged at $600 \times g$ for 25 min. Cells at the 34% Percoll layer (p34; 1.035–1.052 g/L layer) and 51% Percoll layer (p51; 1.064 g/L layer) were collected, washed with RPMI 1640 medium, and subsamples were either stained using a Sudan Black B staining kit (Sigma-Aldrich) or analyzed by flow cytometry on a BD Biosciences FACScan system.

Identification of Ictalurus punctatus *FcRI (IpFcRI)*

Using mammalian FcR sequences CD16, CD32, and CD64 as queries to search the catfish databases, a single EST (BE469704) from a catfish pronephros (head kidney) cDNA library was identified. Subsequently, 3'-

RACE protocols were used to obtain the full-length IpFcRI sequence using the primers listed in Table I. A search for IpFcRI-like sequences among 44,037 ESTs in the TIGR Catfish Release 6.0 database (⟨www.tigr.org⟩) using basic local alignment search tool (BLAST) analysis (47) identified five matching ESTs (CK422401, CK412589, CK405253, CK411364, and BE469529).

A bacterial artificial chromosome (BAC) 059-N02 was identified by PCR screening of the CCBL1 BAC library (48) using the primers listed in Table I. The *IpFcRI* gene was sequenced directly from BAC DNA by primer walking (U.S. Department of Agriculture/Agricultural Research Services Mid South Area Genomics Laboratory, Stoneville, MS). IpFcRI-related sequences in other teleosts were identified by BLAST (47) against the National Center for Biotechnology Information (NCBI; ⟨www.ncbi. nlm.nih.gov⟩) databases. A rainbow trout IpFcRI-related sequence was generated by aligning the following ESTs: CA350052, CA350202, CA354438, CA356126, CA357473, CA344819, CA345217, CA347628, CA359710, CA366579, CA371062, CA372019, CA372368, CA374824, CA381028, CA381525, CA388014, CA366714, CA375361, CA381310, BX082867, BX082868, BX075495, BX075496, and CR374266. A *Tetraodon nigroviridis* IpFcRI-related sequence (CAF97406) was also identified, and a *Fugu rubripes* sequence was found within Scaffold_610.12 using BLAST (⟨www.genome.ucsc.edu⟩) and Genscan Gene predictions.

Sequence analyses

Nucleotide and amino acid sequences were analyzed using DNASTAR softwareand aligned using CLUSTAL_W (49). Neighbor-joining trees with pairwise gap deletions were drawn using MEGA v3.0 (50). Similarity searches were performed using BLAST (47) against the NCBI nonredundant protein database and the Protein Data Bank (PDB). Ig domains, TM segments, and secondary structure were predicted using Simple Modular Architecture Research Tool (51), Pfam databases (52), and the 3D-PSSM server (53). Signal peptide and predicted signal peptidase cleavage site was performed using the SignalP 3.0 server (⟨www.cbs.dtu.dk/services/ SignalP⟩). Sequence decorations were performed using GeneDoc (⟨http://psc.edu/biomed/genedoc⟩). Protein modeling was performed using SWISS-Model (⟨http://swissmodel.expasy.org//SWISS-MODEL.html⟩). The GPI-anchorage prediction program, big-PI Predictor, was used to locate potential GPI-anchorage sites (⟨http://mendel.imp.univie.ac.at/ gpi/gpi_server.html⟩).

Southern blot and expression analyses

Genomic DNA was prepared using erythrocytes from outbred catfish (54), and 10 μg was digested with *Pst*I or *EcoR* I, separated on 1% agarose gels, and transferred to Hybond-N+ membranes (Amersham Biosciences). Hybridizations were performed in Rapid-Hyb buffer (Amersham Biosciences) at 65°C, and membranes were washed at high stringency (65°C with 0.1X SSC, 0.1% SDS). The 5′ IpFcRI probe consisted of the first two Ig domains of IpFcRI, and was PCR amplified using primers I317F and I318R (Table I) with IDPol DNA polymerase (ID Labs Biotechnology) and random primed with ^{32}P-labeled dCTP by Megaprime labeling (Amersham Biosciences). The 3′ IpFcRI probe (primer pairs I265F and I271R; Table I) contained part of the third Ig domain plus the untranslated (UT) region. For Northern blots, total RNA from catfish PBL, cell lines, and various tissues was prepared using RNA-Bee (Tel-Test); 10 μg of each sample were electrophoresed on 1.5% formaldehyde-agarose gels and transferred onto Hybond-N+ (Amersham Biosciences), hybridized, and washed as above.

For RT-PCR, freshly isolated RNA was treated with DNase I (Invitrogen Life Technologies), and 1 μg was converted into cDNA using an oligo-T primer and 200 U Superscript III RT (Invitrogen Life Technologies). Amplification was performed using catfish-specific primers listed in Table I. Typical parameters were as follows: 3 min 94°C, followed by 30 cycles of 94°C 30 s, 58°C 30 s, and 72°C 1 min 30 s, with a final 10 min extension at 72°C. Products were visualized on 1.2% TAE-agarose gels. Quantitative (q)PCR was performed using the iCycler iQ (Bio-Rad) in 96-well microtiter plates. Reactions contained 12.5 μl SyberGreen Master Mix (100 mM KCl, 40 mM Tris-HCl (pH 8.4), 0.4 mM each dNTP, 0.5 U iTaq DNA polymerase, 6 mM MgCl$_2$, 20 nM SyBrGreen dye; Bio-Rad), 1 μl of each forward and reverse primer (0.2 μM), 1 μl of template, and 10.5 μl of H$_2$O. All samples were amplified in triplicate. The cycling protocol was 2 min 95°C, followed by 40 cycles of 95°C 25 s, 57°C 30 s, and 72°C 20 s. A negative control devoid of template was included for each primer pair. Amplification efficiencies were calculated from standard curves generated using four 10-fold serial dilutions of catfish cDNA. The relative expression ratio was calculated by the comparative C_t method using 18S as an endogenous control and cDNA derived from unfractionated PBL as a reference.

Recombinant protein expression and binding of IgM to IpFcRI

To assess IgM binding capabilities of IpFcRI, recombinant proteins were generated using both prokaryotic and eukaryotic expression systems and tested in Ig-binding assays. rIpFcRI was produced in *Escherichia coli* by cloning the three IpFcRI Ig domains into the Champion pET 100 Directional TOPO expression vector (Invitrogen Life Technologies). The rIpFcRI, containing an N-terminal 6xHis epitope tag, was purified using MagneHis Ni-Particles (Promega) according to the manufacturer's protocol, and refolding was performed according to the protocol given in the protein refolding kit (Novagen). The rIpFcRI was ~34.6 kDa, including an ~4.1-kDa epitope tag, and was detected by the anti-Xpress mAb specific for the N-terminal Xpress epitope.

For the coimmunoprecipitation of catfish IgM with rIpFcRI (or rIpFcRI with catfish IgM), 2.5 μl of CFS was diluted in 500 μl of immunoprecipitation (IP) buffer (50 mM Tris-HLC, 300 mM NaCl, 0.1% SDS pH 7.5) and precleared with 20 μl of Sepharose G beads (Amersham Pharmacia Biotech) for 30 min at 4° C. Two μg of rIpFcRI, 25 μl of Sepharose G beads, and 1 μg of anti-Xpress mAb or 1 μg of anti-V5 mAb (Invitrogen Life Technologies) were added to the precleared CFS and incubated for 14 h at 4°C on a rotary shaker. Immunoprecipitations were also performed as described above but with 50 μl of anti-catfish IgM mAb 9E1 or 50 μl of the isotype control mAb (1.14). After three washes, the Sepharose G beads were re-suspended in 75 μl of IP buffer and 25 μl of 4X SDS-PAGE reducing buffer and boiled for 5 min. Twenty μl samples were electrophoresed on 10% SDS-PAGE gels, transferred to Hybond-ECL nitrocellulose membranes (Amersham Biosciences) and incubated in Tris-buffered saline supplemented with 1.0% BSA and 0.1% Tween 20 (TTBS-BSA) for 30 min at room temperature. Duplicate membranes were incubated overnight with either anti-catfish IgM mAb 1H12 (1/2 v/v) or anti-Xpress mAb (1/5000 v/v) in TTBS-BSA for the detection of catfish IgM and rIpFcRI, respectively. Following incubation with primary Abs, membranes were washed and incubated for 1 h at room temperature with 1/5000 (v/v) of goat anti-mouse Ig (H+L)-HRP (Southern Biotechnology Associates) diluted in TTBS-BSA. After a final wash in TTBS, immunoreactive bands were detected using the SuperSignal West Pico chemiluminescent substrate kit (Pierce).

To verify the Ig-binding results obtained with *E. coli*-produced protein, IpFcR also was expressed on the surface of HeLa cells. Briefly, an IpFcRI fragment encoding the three Ig domains was amplified from spleen cDNA using primers incorporating an *Xma*I site before the first Ig domain and a *Pst*I site after the third Ig domain (Table I). This IpFcRI product was then cloned into the pDisplay vector (Invitrogen Life Technologies) that introduces an N-terminal Ig κ-chain leader sequence and C-terminal platelet-derived growth factor receptor (PDGFR) TM segment designed to target the protein to the cell surface. The IpFcRI-PDGFR construct was then transiently expressed in HeLa cells using GeneJuice Transfection Reagent (Novagen) according to the manufacturer's protocol. After 48 h, surface expression was detected by flow cytometry using anti-c-*myc*-FITC conjugated mAb (2 μg/ml; Sigma-Aldrich) and by immunoprecipitation using the anti-HA mAb (HA.11 ascites fluid; Covance) as described previously (55). To determine whether surface expressed IpFcRI binds catfish Ig, IpFcRI-transfected HeLa cells were incubated with either 1% CFS or 25 μg/ml purified catfish IgM (56) for 20 h at 37°C. Cells (1 × 10^6/ml) were harvested and washed with ice-cold RPMI 1640 medium containing 0.3% sodium azide, and 100 μl of the cell suspension was incubated with 100 μl of a 1/2 dilution of mAb 9E1 (for surface IgM detection) or mAb 1.14 (negative control) for 30 min. After washing, cells were incubated with 15 μg/ml goat anti-mouse Ig (H+L)-biotin (Southern Biotechnology Associates) and 10 μg of streptavidin-PE (BD Biosciences) for 30 min each. Detection of IgM (9E1) reactive HeLa cells was determined by analyzing samples on a BD Biosciences FACScan.

Secretion and detection of native IpFcRI

To test whether the native leader of IpFcRI could generate a secreted protein, IpFcRI was amplified using primers incorporating a *Sac*I site before the native leader and an *Eco*RV site after the third Ig domain (Table I). The product was cloned into the pIB/V5-His (Invitrogen Life Technologies) insect expression vector and then transiently transfected into Sf9 cells (Invitrogen Life Technologies) using Cellfectin reagent (Invitrogen Life Technologies). After 72 h, supernatants (30 μl) and cell lysates were examined for rIpFcRI by Western blot using the anti-V5 mAb.

A rabbit IpFcRI pAb was produced using the *E. coli*-generated rIpFcRI protein according to the protocols of Cocalico Biologicals. Rabbit sera (1/1000–1/10000 (v/v)) were screened by Western blots against the rIpFcRI (~100 ng per lane) using goat anti-rabbit IgG-HRP (1/5000 (v/v); Southern Biotechnology Associates) as the secondary Ab. The prebleed

Table I. *IpFcRI Primers*

Primer	Sequence 5′ to 3′	Location[a]	Use[b]
1266 F	CCGACGAACCACAGAACCAA	317–333	s
1264 F	GTAAGGAGTGGGAACAAAGTGGA	3245–3267	s
1265 F	AAATGGCAACAGGCTAGGACC	3334–3354	s, h
1271 R	AGCCAATCATGCATATGTATTC	4135–4156	s, h
1316 R	AATAGCTGTGTTGCTTCGTGCA	3890–3911	s, p
1317 F	CTCCCGGGACAGTGAGTTTGGGAAAGC	799–817	s, h, c, p, n
1318 R	AGCTGCAGCAGAGACTGGGAAGACTG	2884–2902	s, h, n
1319 R	AGCTGCAGTTTACCTGGTTACTCCACC	3453–3472	s, c, p
1385 F	CTCCCATCCATGTGATCAC	3977–3995	s
1386 F	CCAGGTGAGGAATACACAGA	1939–1958	s
1387 R	CCATGAGGTGGCATGTTGAA	1414–1433	s
1388 F	CATGCCACCTCATGGCAAAG	1419–1438	s
1389 R	CACTTAGGGGTGTACTCGCT	1246–1265	s
1390 R	GGGTTTAGGTCTGGAGACAT	2168–2187	s
1391 R	CTTTCCCAAACTCACTGTGGCAA	796–816	s
1392 F	GACCCTCTTAAAATACATGTTGA	1036–1058	s
1393 R	ATGTGCCAACACTGAAGAAATGA	2451–2563	s
1394 F	ATCAGTCTTCCCAGTCTCTGC	2882–2902	s
IpFcRI pIB F	ATAGGAGCTCAGGCAACGCAACCACCATG	334–352	i
IpFcRI pIB R	TTTGATATCGTTTACCTGGTTACTCCACCG	3452–3472	i
IpFcRI-RT F	TGCCAGAGACACATACGCCATC	3361–3382	q
IpFcRI-RT R	CCAAGGTCTACAGGTTCAGAGGAG	3486–3509	q
18S-RT F	CGCCCCGCCCAACTCGCCTGAATA	N/A	q
18S-RT R	CGAATGCCCCCGCCGTCCCTCTTA	N/A	q
TCRα F	CGGGAGCCGTCAATTTACAAA	N/A	p
TCRα R	GCAGGCAAATGAAAGTAGAAT	N/A	p
IgμM F	GAGTGGATCAATGGCACCGAATTCAT	N/A	p
IgμM R	CTCCATCTCATAGTGGAAGATCTCTG	N/A	p
EF1α F	GACTGCCACACTGCTCACATTG	N/A	p
EF1α R	TTAGTTACTCAGCAGCTTTCTTCC	N/A	p

[a] Refers to nucleotide number in GenBank DQ286289.
[b] s, Sequencing; h, hybridization; c, protein expression; p, RT-PCR; n, nested PCR; i, insect expression; q, qPCR.
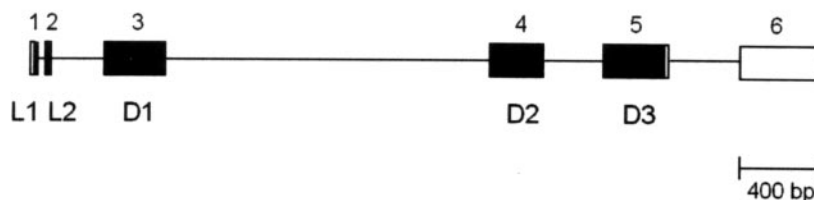
A

```
                                                         CCGACGAACCACAGAACCAAAGGCAACGCAAGCCACC        37
                                                         >
<Signal Peptide
ATGCACTTTTTCCACATCCTTCATCGTTTTTATAACATTGCTTGCATGTGTCAGGATGGATGATATAGATCCCACACCACCCCCAGTGAAA    127
 M  H  F  F  H  I  F  I  V  F  I  T  L  L  A  C  V  R  M  D  D  I  D  P  T  P  P  P  V  K
                                                      < Domain 1
GCCAAAGCCACAGTGAGTTTGGGAAAGCCGCGGCTGTTCTCAGGGGAAGATGTGCAGATGACTTGCAGTGTCCCAGATGACCCTTCATCC    217
 A  K  A  T  V  S  L  G  K  P  R  L  F  S  G  E  D  V  Q  M  T  C  S  V  P  D  D  P  S  S

AACTGGACGTATGAGTGGTTCCATGATGGTGAACTCTTGAGCGCCACAGAAGTGTACAGTTTAAACAAGGCACAAGTCCTGCAAAGTGGA    307
 N  W  T  Y  E  W  F  H  D  G  E  L  L  S  A  T  E  V  Y  S  L  N  K  A  Q  V  L  Q  S  G
                                                                                       >
AACTATACCTGTAAAGGATTGAAGACGATAAAAGCTTGGCCCTATATAGTGCCATCAATTCCAAGCGACCCTCTTAAAAATACATGTTGAT   397
 N  Y  T  C  K  G  L  K  T  I  K  A  W  P  Y  I  V  P  S  I  P  S  D  P  L  K  I  H  V  D
< Domain 2
GGTGGTTGGGTTCTCCTACAAACCCCATTTGAGCCATTAATTATTGAGGAAAACATGACTCTGACCTGCCGTGTCCGTGATGACCCCCTC    487
 G  G  W  V  L  L  Q  T  P  F  E  P  L  I  I  E  E  N  M  T  L  T  C  R  V  R  D  D  P  L

CTGTCAAATGTGATCTTCTACAAGGATGGGGTGGAGTTCAATAAGCAGAAAGGCACAGATGTGGTGTTCACCAAACTCACGCTTGAGGAT    577
 L  S  N  V  I  F  Y  K  D  G  V  E  F  N  K  Q  K  G  T  D  V  V  F  T  K  L  T  L  E  D
                                                                                       >
GCTGCCATTTACTCATGCAGGGCCACATGGATTAAGAACATGGAATATCAGTCTTCCCAGTCTCTGCCTTCTTATGTGACTGTATTAGAT    667
 A  A  I  Y  S  C  R  A  T  W  I  K  N  M  E  Y  Q  S  S  Q  S  L  P  S  Y  V  T  V  L  D
                              < Domain 3
ATATTGGAAACACCCACGATGACGATTGTCGGAGGTCGGGGTAGAGTAAGGAGTGGGAACAAAGTGGAATTCAGATGTATTACCAAAGTA    757
 I  L  E  T  P  T  M  T  I  V  G  G  R  G  R  V  R  S  G  N  K  V  E  F  R  C  I  T  K  V

AATGCTAGAGAACAAGACCTGAATATAGAATACTTCTACTTAAAAAATGGCAACAGGCTAGGACCTGCTTCTGCCAGAGACACATACGCC    847
 N  A  R  E  Q  D  L  N  I  E  Y  F  Y  L  K  N  G  N  R  L  G  P  A  S  A  R  D  T  Y  A
                                                                                  >
ATCTCAGAGGTGAACATAAATCATACCGGAAACTACACCTGCAAAGTCCGTATAAGGGCTCTGAATGTGGAGCGGTGGAGTAACCAGGTA    937
 I  S  E  V  N  I  N  H  T  G  N  Y  T  C  K  V  R  I  R  A  L  N  V  E  R  W  S  N  Q  V

AACCTGAAGGTCCTGCCTCCTCTGAACCTGTAGACCTTGGGATGTAAGTTTCTGAGAGCCAGTGTACCAATGCTCCAGCCCTGGAATGCA   1027
 N  L  K  V  L  P  P  L  N  L  *

CGAAGCAACACAGCTATTCAGCTATCATCCAAGTTCTTCACTATTTTAGAATACTCTTGCATTGTTCACTGTTTTCTGCCTTTCTCCCAT   1117
CCATGTGATCACAATTCTGACCTTTAAACGTATGTTATATACTGGATTGATGATGCAAATTATATTTTGAATCTGAGAAACTTTTTATACC   1207
TTTTATTTCATTTTACAAGAACAGAGATATACCCTTAAATAACAGTTTTCCTATTTGATTTGAATACATATGCATGATTGGCTTATTTAA   1297
ATCTTAAAATGCAATACTATTTTACTTTGGAAACTATGTGTAATAAAGTGTTTTTTTTGTTTTTTTACAATCTCATCAATAAACACATGGAA   1387
CACATGAAAAAAAAAAAAAAA                                                                       1409
```

B

C


```
                  < Signal Peptide      >          < Domain 1
I. punctatus   : M-HFFHIFIVFITLLACVRM---DDIDPTPPPVKAKATVSLGKPRLFSGEDVQMTCSVPDDPSSNWTYEWFHDGELLSAT-EVYSLNKAQVLQSGNYTC : 94
O. mykiss      : MKLLLSLL--VVSTLPQLAE---LQVLPTSAPQTAVAELVKGLPWIFSGESVHLKCSVPGNVSAEWRYRWFRGGEQLQES-EYFVLWKARPQQSGKYYC : 93
F. rubripes    : MEVVVFLLDALKSIFDLLIESSLFPEAPLGAQFRAVLEIVSGHSRIFSGDTDVKLKCNIPDPYQSTWRYLWFKGSEELQQHGNELIIWRARIIDSGKFYC : 99
T. nigroviridis: METVVVFFL-AL-STLPRLSE----PLVNLVAPYNPVVEILSGDTRIFSGEGVAILQCTVPD-HMSTWQYRWFKGSEELHYHGQIFVLWKARVDDTGKSYC : 92

                        > < Domain 2
I. punctatus   : KGLKTIKAWPYIVPSIPSDPLKIHVDGGWVLLQTPFEPLIIEENMTLTCRVRDDPLLSNVIFYKDGVEFNKQKGTD--VVFTKLTLEDAAIYSCRATWI : 191
O. mykiss      : QGLRT--TWINTQHTLHSLPIEIEVDGGWAILQAPPLPMLVGETMTLTCRVRNNPKLTEVILYKDGVELQIQRGPE--LRVTNLTLQHHGSYWCRASWD : 188
F. rubripes    : QGVRD--TAVGQLHTNQSLPVEIFVDGGWALTRVTPQPALVGHTLEVTCLVRGKHPHTEVILYRDGVEVMRERGKDPQFILSNLTTEDQGMYSCRASWD : 196
T. nigroviridis: QGVRD--TVVGDIRTLQSVPVEIIVDGGWALTHVTPQPALVGHSLEVTCRVRGRRPLSEVILYRDGVEVMRNQGNNPKFLLSNLTIEDQGMYSCRASWD : 189

                          > < Domain 3
I. punctatus   : KNMEYQSSQSLPSYVTVLDILETPTMTIVGGRGRVRSGNKVEFRCITKVNAREQDLNIEYFYLKNGNRLGPASARDTYAISEVNINHTGNYTCKVRIRA : 290
O. mykiss      : GRRETNSVISVAAPVSIIEVLTEPMLEIVPNDPLIHK-DRMLLVCHVQLNARQPVPHIHYYFYQDGLSLGPASSQDKITVLRD----SGQYWCKASIPT : 282
F. rubripes    : VRGLTHSVMSVETLGRVVEILTKPVLEIDVNNNQIP--NRMKLICHHEYNLPAPAPPVHFYFYKNDKVLGPATSENRLSVNQR----PGLYSCKKVPVT : 289
T. nigroviridis: TNSQTHSVISVHIPG---------MVRRGSVQTASGDQCCQQLTESQDEARLPTRVKTSRSCPSAAILFLKVKKGAG---------------------- : 256

                  <
I. punctatus   : LNVERWSNQVNLKV-------LPPLNL--------------------------- : 310
O. mykiss      : LGLKRLSKPLGYGRVTGEPSEHLRMRNQKIIVVPL---------------------- : 317
F. rubripes    : PVLVHPHDVATQRSVEPTEASTLPPEVQSLNQTTAAPQTINIPEASGDMSGESGDFTDDDSP-- : 351
T. nigroviridis: ----------------------------------------------------------- : -
```

FIGURE 1. Comparison of catfish IpFcRI and other teleost FcR-like sequences. *A*, Nucleotide and predicted amino acid sequence of IpFcRI. Predicted signal peptide and Ig domains are labeled, the signal peptide cleavage site between residues 19 (M) and 20 (D) is underlined, potential N-linked glycosylation sites are gray shaded, and the stop (TAG) codon is underlined and marked (∗). Polyadenylation sites are underlined and nucleotide numbers are at left. *B*, Schematic IpFcRI gene representation. Exons are numbered and labeled with the regions that they encode: L1 and L2, leader sequence; D1–D3, domains 1–3; ☐, 5′ and 3′ untranslated regions. The GenBank accession numbers for IpFcRI cDNA and the *IpFcRI* gene are DQ286290 and DQ286289, respectively. *C*, Amino acid alignment of IpFcRI with related fish FcR-like sequences. The predicted signal peptide and domains are labeled. Residues similar/identical with IpFcRI are gray shaded; conserved cysteines are boxed, and gaps (−) are indicated. Amino acid numbers are at right.

sera demonstrated no immunoreactivity at all dilutions tested, whereas immune sera readily detected the recombinant protein (data not shown). The IpFcRI pAb (1/3000 (v/v)) was then used to detect IpFcRI in catfish plasma samples (5 μl per lane) by Western blot analyses. For some experiments, the plasma proteins were deglycosylated using PNGaseF (0.01 U; QA-Bio, CA) for 3 h at 37°C according to the manufacturer's instructions.

Results

IpFcRI sequence analyses

By searching the catfish EST databases using the mammalian FcR sequences CD16, CD32, and CD64 as queries, a catfish FcR homolog (IpFcRI) was identified. IpFcRI cDNA consists of 1409 nucleotides with a 933-bp open reading frame encoding 311 aa (Fig. 1A). The polypeptide is composed of a signal peptide sequence containing a signal peptidase cleavage site between residues 19 and 20 (predicted using SignalP 3.0 software) and a 292-aa region containing three Ig-like domains (D1–D3). The mature protein has a predicted weight of 32.77 kDa. Five potential N-glycosylation sites were found, two within the first Ig domain, one in the second Ig domain, and two in the third. The IpFcRI transcript does not encode a TM segment or CYT region. The third Ig domain ends at leucine 290, and the remaining 19 C-terminal amino acids encode a region of low compositional complexity with no identifiable motifs or domains. Notably, no GPI-anchorage prediction sites are predicted within the sequence, suggesting that IpFcRI is secreted. Five additional IpFcRI cDNAs also were identified from the known catfish databases in an attempt to find an IpFcRI-like transcript containing a TM and/or CYT segments. A total of 44,037 ESTs were screened, and all 5 IpFcRI-like sequences were identical with the original IpFcRI and lacked a TM and CYT. Furthermore, cDNA library screens, nested PCR, and 3′RACE protocols yielded only IpFcRI transcripts that lacked TM segments and CYT regions (data not shown).

The *IpFcRI* gene spans 3944 bp and consists of 6 exons (Fig. 1B). The first 33 nucleotides of exon 1 are UT, and the remaining 25 nucleotides plus the first 36 nucleotides of exon 2 encode the predicted leader sequence. Exons 3–5 contain 300 bp, 277 bp, and 328 (305 coding) bp, respectively, each encoding a single Ig domain. The last 60 nucleotides of exon 5 encode the low-complexity region and part of the 3′ UT region. All of the *IpFcRI* exon/intron boundaries follow a phase 1 splicing pattern. Exon 6 encodes the remainder of the 3′ UT. The longest intron, 1596 bp, is between exons 3 and 4.

Database searches and genome mining identified IpFcRI-related sequences in pufferfish and rainbow trout (Fig. 1C). These related sequences were 21–33% identical with IpFcRI and the highest amino acid identities/similarities were present in the D1 and D2 regions. The IpFcRI predicted signal peptide was not similar with those of the other fish species and the *Tetraodon nigroviridis* sequence was truncated within D3. Both the trout and *Fugu rubripes* IpFcR-like sequences appeared to encode full-length proteins, and like catfish, they lacked TM and CYT regions, suggesting that FcR homologs lacking TM and CYT are not unique to catfish.

Phylogenetic analysis and similarity searches

Database searches using the IpFcRI predicted amino acid sequence identified various mammalian FcR and FCRLs as potential relatives (*E* values ranging from 4e-19 to 1e-10; ~25–35% amino acid identity; Table II) a relationship reinforced by phylogenetic analyses. As shown in Fig. 2A, the IpFcRI D1 and D2 Ig-domains (encoded by exons 3 and 4) cluster with high bootstrap values with their mammalian FcR Ig-domain counterparts. IpFcRI D2 also appears to be related to the D2 of a new FcR-related molecule (FcRX) that is also known as the FcR homolog expressed in B cells (FREB; 57, 58). However, mammalian FcRX/FREB does not contain a D1 similar to those of the classical FcR or IpFcRI, a

Table II. *Representative IpFcRI BLASTP Results[a]*

| Receptor		Accession No.	Score	[E] Value
Unnamed	Pufferfish	CAF97406	117	3e-25
FcγRI	Mouse	ABAD97676	98	4e-19
FcγRI	Rat	XP_215643	90	8e-17
XFL1.6	Xenopus	AAQ63873	90	1e-16
XFL1.4	Xenopus	AAQ56585	86	1e-15
FcγRI	Macaque	AAL92095	84	4e-15
FcγRI	Dog	BAC80263	84	7e-15
FcγRI	Human	CAI12557	82	3e-14
XFL1.2b	Xenopus	AAQ56583	80	8e-14
FCRL3	Human	CAH73059	72	2e-11
LITR3	Zebrafish	XP_694305	72	2e-11
LITR1	Catfish	AAW82352	70	1e-10
FcγRI	Bovine	NP_776963	69	1e-10
FcεRIα	Mouse	NP_034314	69	2e-10
LITR3	Catfish	AAW82354	67	7e-10
FcεRIα	Sheep	CAB40544	66	2e-9
FREB-2	Human	AAX11390	66	2e-9
XFL1.1b	Xenopus	AAQ56584	66	2e-9
FcγRIII	Pig	Q28942	65	3e-9
FREB-2	Mouse	AAS82875	62	3e-8
FcγRIII	Bovine	CAA68026	60	9e-8
FcγRIII	Human	NP_000561	60	1e-7
FcRX	Mouse	AAM97592	60	1e-7
FCRL6	Human	NP_001004310	59	1e-7
FcγRIIB	Mouse	AAA97464	54	5e-6

[a] Similarity search (BLASTP) of NCBI's non-redundant protein database using the predicted amino acid sequence of IpFcRI (11/1/05).

notion further reinforced by phylogenetic analysis (Fig. 2A). Neither IpFcRI D1 nor D2 clustered with FcγRI D3 domains or with the two Ig domains of FcαR (CD89), a receptor encoded within the LRC on chromosome 19q13.4. The IpFcRI D3 Ig-domain also was not phylogenetically related to any of the mammalian FcR Ig domains (data not shown). When the IpFcRI D1/D2 sequence was compared with the D1/D2 aa sequences of representative mammalian FcR, FCRL, and with receptors found within the LRC, it was clear that the putative IpFcRI Ig-binding unit was significantly related to the mammalian FcR and FCRL families (bootstrap value = 94; Fig. 2B). Furthermore, IpFcRI D1/D2 is a closer relative to mammalian FcR than are the newly described IpLITRs from catfish, which also encode FcR-related D1 and D2 Ig domains (59). Schematic comparisons of IpFcRI Ig domains with representative mammalian FcR and FCRL (60) as well as IpLITRs are summarized in Fig. 2C.

IpFcRI structural analysis

The predicted β-strand in IpFcRI are present in similar positions as the β-strand found in the mammalian FcR family members with the exceptions of an additional β-strand predicted within the D1 between the F and G strands as well as a missing C' β-strand within the D2 (Fig. 3A). In some instances, the predicted IpFcRI β-strand were present in regions of high amino acid identity/similarity, and five of the FcR residues known to contact the Fc portion of mammalian Ig were either conserved or similar in the catfish sequence (Fig. 3A; note that human FcεR was the FcR used for comparison of contact residues). Similarity searches against NCBI's PDB also revealed that IpFcRI D1 and D2 are structurally related to the corresponding Ig domains of several mammalian FcR. Human FcεRIα (1J89; score 63, *E* value 8e-11) was identified as the closest structural relative to IpFcRI; Fig. 3B depicts a tube diagram comparing IpFcRI and FcεRIα. A protein model of IpFcRI generated using the SWISS-Model program is also shown (Fig. 3B). Similar to FcR, IpFcRI D1D2 folded into two Ig-like domains consisting of eight β-strand that were arranged perpendicular to each other. Such a

FIGURE 2. Phylogenetic analyses reveal IpFcRI contains Ig domains related to mammalian FcRs. *A*, Comparisons of IpFcRI individual D1 and D2 sequences (gray, underlined) with representative mammalian FcR and FcRX/FREB D1 and D2 sequences. *B*, Comparisons of IpFcRI D1D2 (gray, underlined) with representative D1D2 of FcR, FCRL, IpLITRs (gray) and genes encoded by the mammalian and avian LRC. Accession numbers for the Ig domain sequences are: human (hu)FcγRI(CAI12557), huFcγRII (CAA35642), huFcγRIII (CAA36870), huFcεRI (AAH05912), huFCRL3 (AAH28933), huFCRL4 (AAK93970), huFCRL5 (NP_112571), huFcαR (AAH27953), huLILRB1 (AAH15731), huKIR3DL1 (AAC83928), huKIR3DS1 (AAV32446), human NKp46 (AJ001383), mouse (mo)FcγRI (AAD34931), moFcγRII (AAA37608), moFcγRIII (NP_034318), moFcεRI (NP_034314), moFCRL3 (AAS91578), moNKp46 (AJ223765), rat (ra)PIRA1 (XP_341773), CHIRA2 (CAG33731), catfish (Ip)LITR1 (AAW82352), IpLITR2 (AAW82353), and IpLITR3 (AAW82354). *C*, Schematic representation of IpFcRI compared with representative catfish IpLITR, human FcR and selected FCRL. The individual Ig domains for each receptor are shaded according to their relatedness with huFcγRI. Domains colored black have no phylogenetic relationship with huFcγRI.
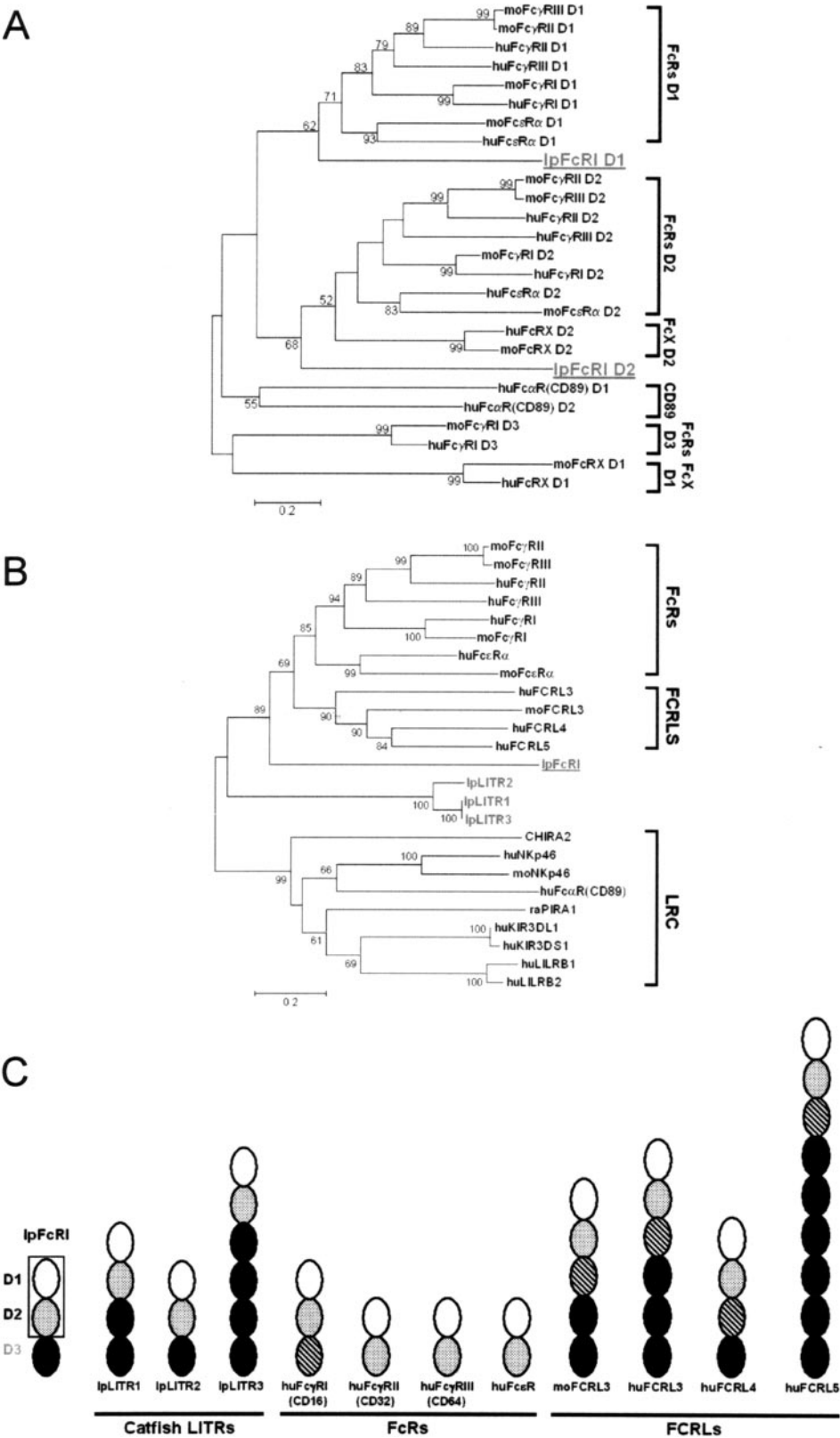
structure is reminiscent of the tertiary protein structure of mammalian FcR determined by crystallization studies (61–63).

Southern blot and expression analyses

Southern blot analysis indicated that the *IpFcRI* is likely a single copy gene (Fig. 4*A*). Only one hybridizing band of ~4kb was observed in *Eco*RI digests with both an IpFcRI D1D2 and a 3′-end specific probe. Comparatively, three bands are observed in *Pst*I digests, which reflect the presence of intronic *Pst*I sites (data not shown). At the message level, IpFcRI transcripts were readily detected by Northern blot (Fig. 4*B*) in spleen, hemopoietic kidney tissues, and PBL. The lower levels of IpFcRI
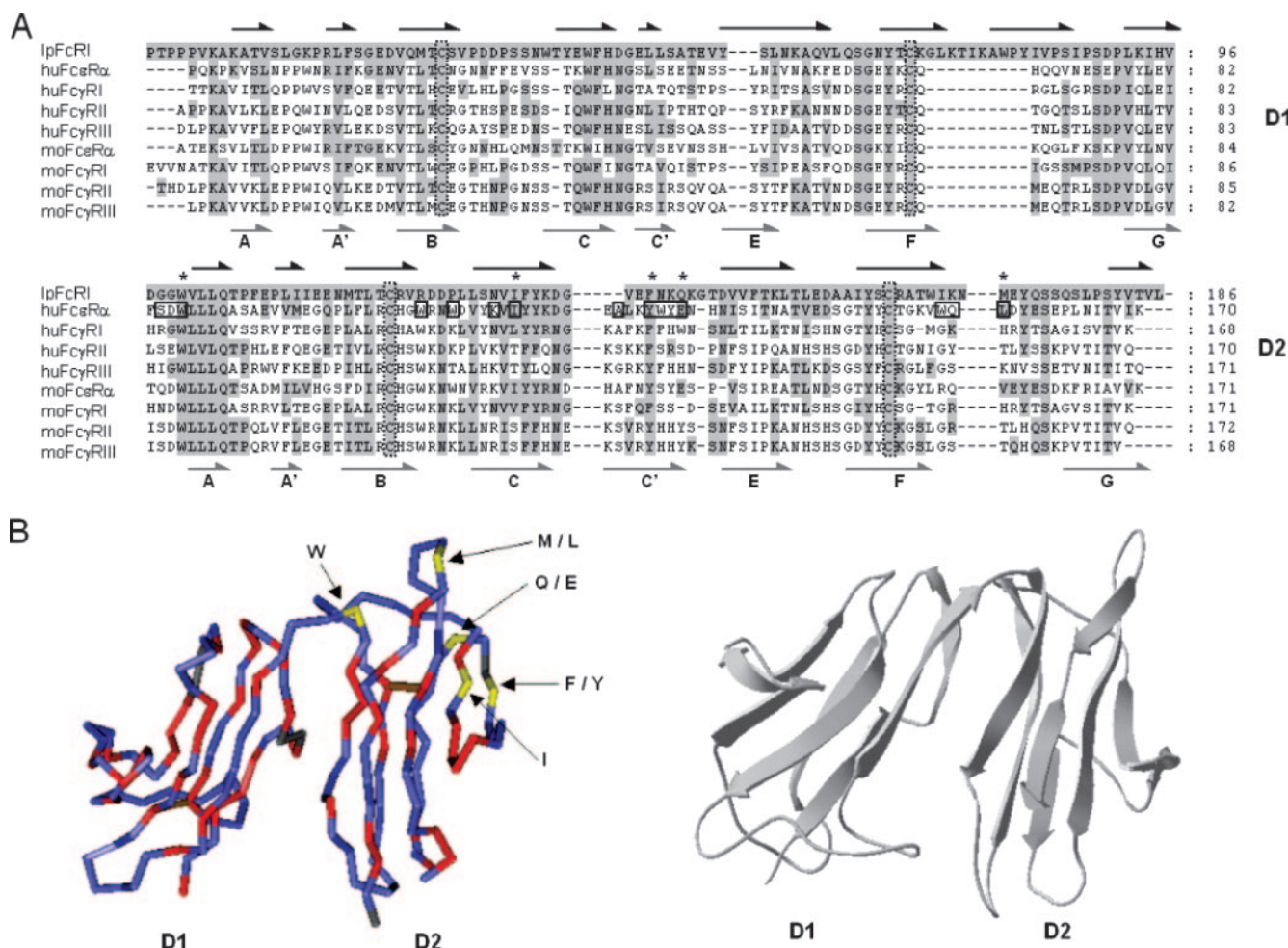
FIGURE 3. Sequence and structural conservation between IpFcRI and mammalian FcRs. *A,* Amino acid alignment of IpFcRI D1 and D2 with representative murine and human FcR D1 and D2 Ig domains. Residues similar/identical with IpFcRI are gray shaded. Residues known to make contact with Ig for the huFcεRIα (**62**) are boxed and (∗) marks residues in IpFcRI that are similar/identical with those contacts. Black and gray arrows represent the predicted β-strand for IpFcRI and huFcεRα, respectively. Hatched boxes indicate conserved cysteines and dashes (−) represent gaps. *B,* Structural comparison of IpFcRI D1D2 with huFcεRI (PDB; 1RPQD, *left panel*). Colors indicate positions where IpFcRI is identical (red), nonidentical (blue), and the location of conserved or similar amino acids involved in contacting the Fc portion of Ig between IpFcRI huFcεRI (yellow). Predicted tertiary structure model of IpFcRI was generated using SwissModel with mouse FcεR (SwissProt Accession No. P20489) as template (*right panel*). Accession numbers for the FcRs used in amino acid alignment are as in Fig. 2.

message expressed in heart, gill, and liver may be due in part to residual PBL in these tissues. Because sFcRs in mammals are released from activated neutrophils, catfish neutrophils were enriched from freshly isolated PBL by depleting IgM-positive cells using MACS and fractionation on a discontinuous 34 and 51% Percoll gradient (Fig. 4C). FACs analysis demonstrated an enrichment of the granular cell subpopulation from ~65% in total leukocytes to ~88% following enrichment (Fig. 4C). The cells present in the lymphocyte gate (based on forward and side scatter analyses) were reduced from 30 to 5% (Fig. 4C). Staining of the neutrophil enriched population with Sudan Black B and enumeration confirmed that these cells were ≥~90% neutrophils. Importantly, analysis by RT-PCR demonstrated that although levels of TCR and μM message were greatly reduced in the neutrophil-enriched fraction, equivalent levels of IpFcRI message were found when compared with the unfractionated PBL. qPCR was performed to assess the expression of IpFcRI in fractionated PBL as well as in various tissue subpopulations. Overall, kidney leukocytes expressed the highest levels of IpF-cRI message when compared with PBL, spleen, gill, and liver

(Fig. 5A). Because this expression was only partially attributed to the IgM-positive subpopulation, the IgM-negative leukocytes were subsequently examined for IpFcRI expression following isopycnic separation on Percoll gradients (Fig. 5B). These experiments demonstrated that IgM-negative lymphocytes (p34 layer) derived from the kidney tissues expressed the majority of IpFcRI with lower levels of expression in the granulocytes (p51 layer). Conversely, within PBL, the granulocytes present at the p51 layer predominantly expressed IpFcRI, whereas IgM-positive cells and the IgM-negative lymphocytes from the p34 layer expressed lower levels of message. Therefore, depending on the tissues examined, the various leukocyte subpopulations differentially expressed IpFcRI.

IpFcRI message expression also was determined in the catfish clonal cell lines, including those representing B cells (3B11 and 1G8), macrophage (42TA), T cells (TS32.17), and a polyclonal MLC (SV12). As opposed to freshly isolated PBL, all cell lines, except for the cytotoxic T cell line TS32.17, did not express detectable message for IpFcRI, nor did a polyclonal MLC (Fig. 5C). However, reamplification from the diluted PCR templates
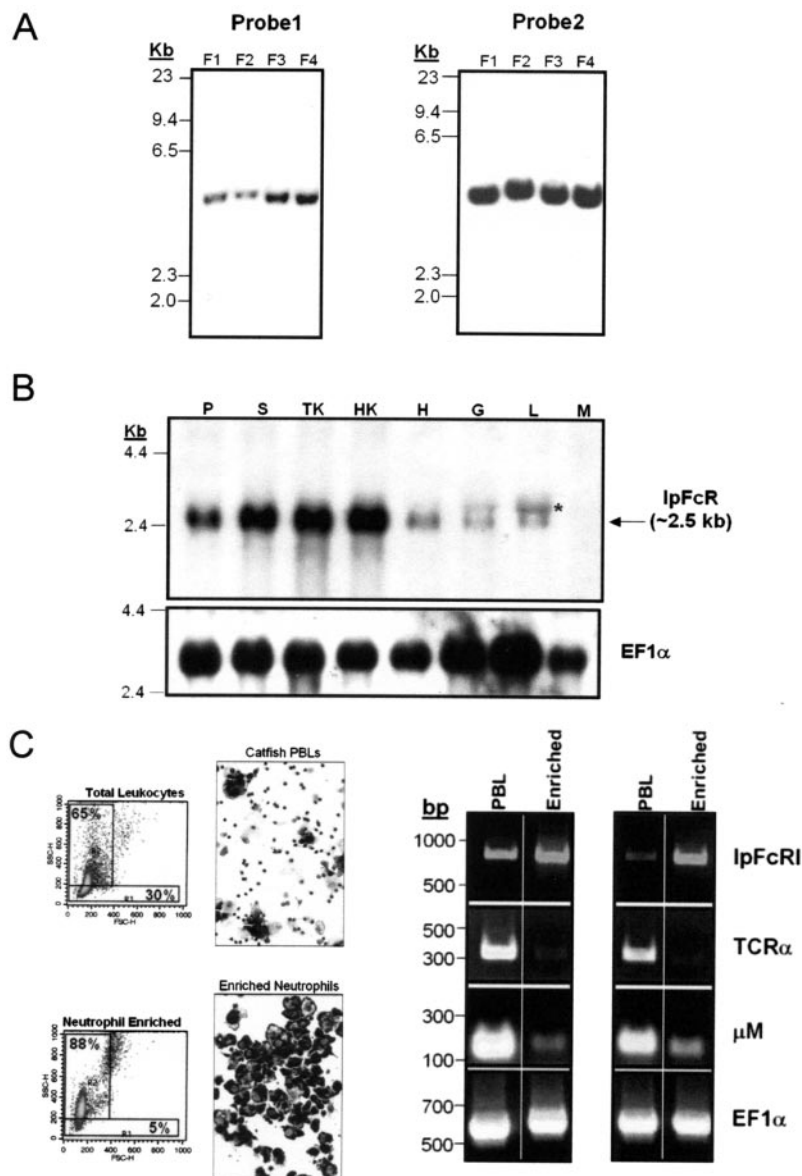
FIGURE 4. IpFcRI gene and expression analyses. *A*, Southern blot analysis using two different IpFcRI-specifc probes is shown. Genomic DNA from four outbred catfish (F1–F4) were hybridized with either an IpFcRI D1D2 (probe 1) or the IpFcRI 3′-end (probe 2). *B*, Northern blot analyses of IpFcRI tissue expression. Total RNA from spleen, pronephros (HK), mesonephros (TK), heart (H), gill (G), liver (L), muscle (M) and PBL (P) were examined. RNA integrity and load levels were determined by using a catfish EF1α probe as a representative housekeeping gene. Kb markers are at the left margin. (∗) marks nonstripped (residual) EF1-positive band. *C*, FACs analysis, Sudan Black B staining of catfish PBL and neutrophil-enriched fractions (40×) and IpFcRI message expression in catfish PBL and neutrophils. RNA was obtained from freshly isolated PBL and neutrophils that were enriched from the same PBL. RT-PCR was performed using primers specific for IpFcRI (I317 F and I316 R), catfish TCRα, IgM H chain (membrane form, μM) and IpEF1α. The panels represent results from two different catfish. Reactions performed without the addition of template failed to amplify products for any of the primer pairs used (data not shown).

revealed that low levels of IpFcRI message could be amplified from 42TA, 3B11, and 1G8 cells, as well as the polyclonal MLC, indicating that in vitro IpFcRI expression is significantly down-regulated, compared with in vivo expression levels (described above).

In vitro secretion of IpFcRI and detection of the native protein

To address the possibility that IpFcRI is a secreted protein it was cloned into an insect expression vector with its native leader peptide sequence and then transiently transfected into an insect cell line (Sf9). As shown in Fig. 6A, rIpFcRI (~52 kDa) was detected in the supernatant of IpFcRI-transfected cells but not in the control, indicating that the native leader can indeed be used to generate a soluble IpFcRI.

Two immunoreactive bands were readily detected in catfish plasma using a rabbit polyclonal anti-IpFcRI with approximate weights of 64 and 90 kDa (Fig. 6B, *left panel*). Both proteins are larger than the predicted weight of the polypeptide (~33 kDa); however, 5 N-linked glycosylation sites identified within the IpFcRI may account for this discrepancy. Following PNGase F treatment, the 64-kDa band was reduced to ~40, 50, and 55 kDa,

which is remarkably similar to the pattern observed following deglycosylation of mammalian soluble FcR (21). The ~90-kDa protein was reduced to ~70 kDa following treatment with PNGase F. Whether or not this is a highly glycosylated form of IpFcRI, a related protein, or a product of nonspecific reactivity to the pAb is presently unknown. Similar-sized bands were detected in PBL lysates (data not shown).

Ig-binding assays

Normal CFS was incubated with *E. coli* generated rIpFcRI and the anti-Xpress mAb in the presence of Sepharose G beads. As demonstrated by Western blot analyses of the immuno-selected material using anti-catfish IgM, anti-Xpress mAb coimmunoprecipitated rIpFcRI with more catfish IgM than did the irrelevant anti-V5 mAb used as a control indicating that rIpFcRI associated with catfish IgM (Fig. 7A, *left panel*). The weak catfish IgM signal observed in the control sample may be due to nonspecific association of residual IpFcRI to the Sepharose G beads because low levels were detected in this sample when developed with the anti-Express mAb (Fig. 7A, *right panel*). Immunoprecipitations using 9E1 mAb not only selected catfish IgM (Fig. 7B, *left panel*), but

FIGURE 5. qPCR of leukocyte subpopulations and IpFcRI expression in catfish clonal leukocyte cell lines. *A*, Determination of IpFcRI expression by qPCR in total leukocytes (■) and Ig⁺ leukocytes (□) derived from PBL and various tissues. The relative amounts of IpFcRI mRNA were measured by qPCR and 18S served as an endogenous control. cDNA derived from unfractionated PBL was used as a reference and arbitrarily set to 1.0. Results are from one representative experiment. *B*, qPCR analysis of leukocytes, Ig⁺, Ig⁻ p34, and Ig⁻ p51 leukocyte subpopulations derived from PBL (■), pronephros (HK; ▨), and mesonephros (TK; □). Individual bars represent the mean plus SD calculated from three replicate experiments using cDNA from an individual fish. *C*, IpFcRI RT-PCR and nested PCR expression analyses in various catfish clonal cell lines, PBL and MLC (SV12). IpFcRI specific primers I317 F and I316 R were initially used in PCR (*top panel*). The PCR were diluted 1/100 (v/v) and then re-amplified with the specific primers I317 F and I319 R (see Table I). PCR products were verified by sequencing and PCR performed without the addition of template failed to amplify products for any of the primer pairs used (data not shown).
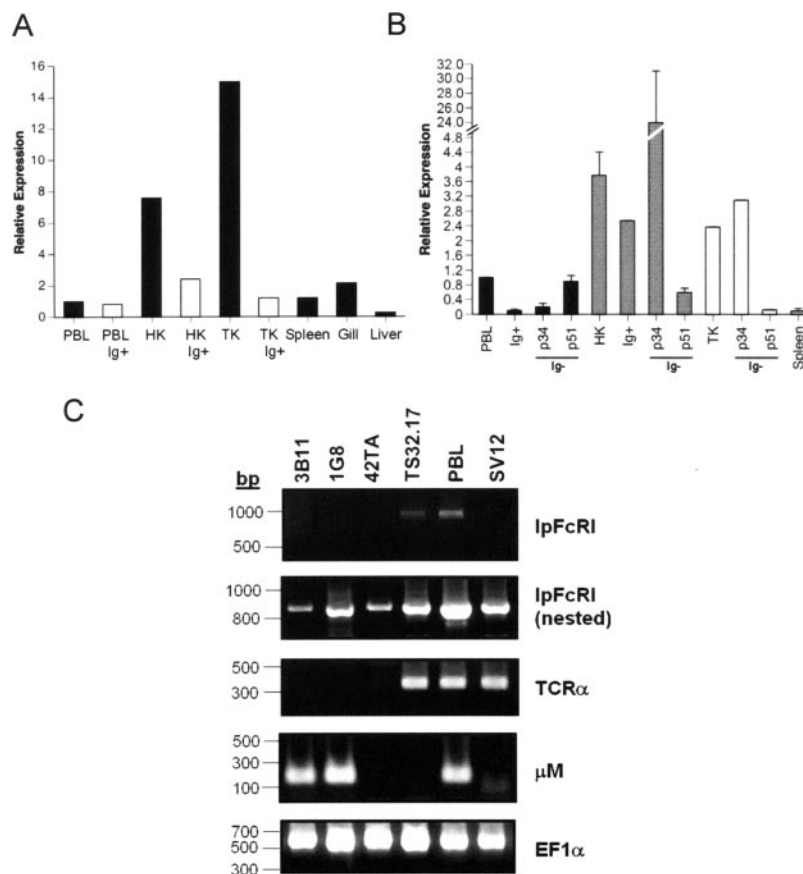
also coimmunoprecipitated rIpFcRI (Fig. 7*B*, *right panel*), again suggesting that rIpFcRI binds to catfish IgM. Neither catfish IgM nor rIpFcRI were detected when replicate experiments using 1.14 (isotype control) were performed (Fig. 7*B*).

To verify the binding results obtained with prokaryotic produced protein, IpFcRI also was cloned into the eukaryotic pDisplay expression vector. The IpFcRI-PDGFR construct, which contains myc and HA tags, was transiently expressed in HeLa cells, and the cells were then incubated with CFS or purified catfish IgM. Surface expression of IpFcRI was demonstrated by increased anti c-myc reactivity and an average of 40% of the cells exhibited increased staining (i.e., percent increase of FL1 staining vs mock-transfected cells) 48 h posttransfection (Fig. 8*A*, *upper panel*). To verify the FACS results, IpFcRI was subsequently immunoprecipitated from the HeLa cells using the anti-HA mAb and detected by Western blot (Fig. 8*A*, lower panel). An immunoreactive band of ~42 kDa that was equal to the predicted M_r of IpFcRI plus the epitope tags and the PDGFR transmembrane segment encoded by the pDisplay vector was detected in the IpFcRI-transfected HeLa cells and not in the mock-transfected cells (Fig. 8*A*, *bottom panel*). Subsequently, incubation of the IpFcRI-transfected cells with 25 μg/ml catfish IgM or 1% CFS resulted in increased and equivalent intensity of mAb 9E1 staining, 72 and 68%, respectively, compared with mock-transfected cells and isotype (1.14) controls (Fig. 8*B*). These results indicate that catfish IgM preferentially associated with the transfected cells by reacting with the surface expressed IpFcRI and that other proteins found in CFS likely do not competitively inhibit the binding of catfish IgM to IpFcRI.

Discussion

In the present study, a novel catfish FcR cDNA, termed IpFcRI, is characterized. It consists of three predicted C2 Ig-like do-

mains with no identifiable TM/CYT segments or GPI-linkage motif(s), suggesting that IpFcRI is secreted and/or intracellularly expressed. The *IpFcRI* gene consists of six exons that encode a split leader peptide (exons 1 and 2), three Ig-like domains (exons 3–5), as well as a UT region (exon 6). The first five exons follow a phase 1 splicing pattern and in combination with the split leader peptide; the *IpFcRI* gene shares features characteristic of other FcR family members (5, 20). Although IpFcR lacks TM/CYT, it may have significant functional roles in teleosts as a sFcR. Soluble FcR in mammals inhibit the binding of immune complexes to FcγR-positive cells, down-regulate B cell proliferation and Ab production, and trigger cellular activation by binding complement receptors (19, 21, 24–26). Both alternative splicing mechanisms and proteolytic cleavage of the membrane FcR have been shown to produce sFcR. At present, the functional significance of IpFcRI as a soluble protein is unknown; however, we have demonstrated that IpFcRI can be secreted in vitro using its own leader peptide, and the endogenous protein was detected in catfish serum/plasma with a pAb. This evidence reinforces that IpFcRI does indeed exist in vivo as a soluble protein. As in mammals, several N-linked glycosylation sites are present throughout the IpFcRI sequence. Phylogenetic analyses and similarity searches revealed that in addition to an unnamed pufferfish sequence (CAF97406), the majority of IpFcRI-related proteins were mammalian FcR and FCRL family members (e.g., mouse FcγRI, *E* value 4e-19; 26% amino acid identity) as well as several XFL and the three IpLITR-types. However, unlike the multigene and highly diversified *XFL* and *IpLITR* gene families (59, 64), only a single gene encodes IpFcRI.
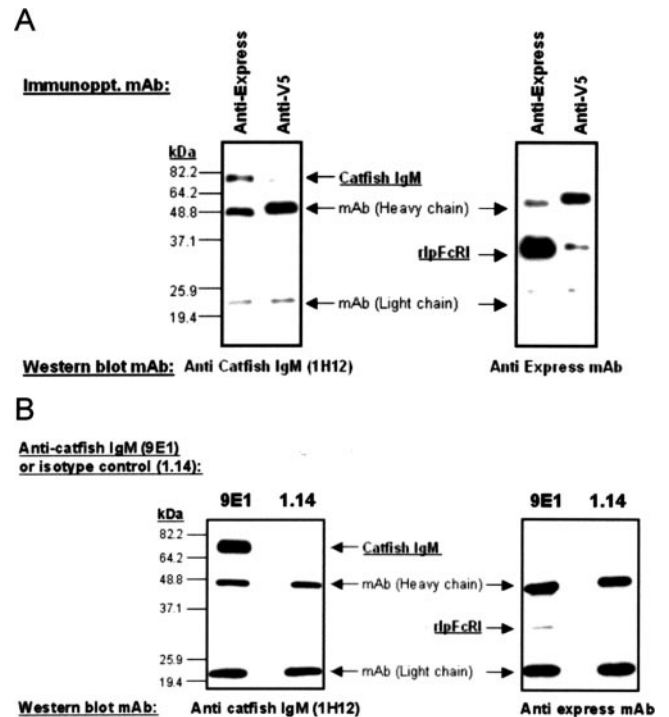
IpFcRI is expressed primarily in catfish lymphoid tissues, with much lower levels of expression found in nonhemopoietic tissues such as heart, gill, liver, and muscle. Following separation into
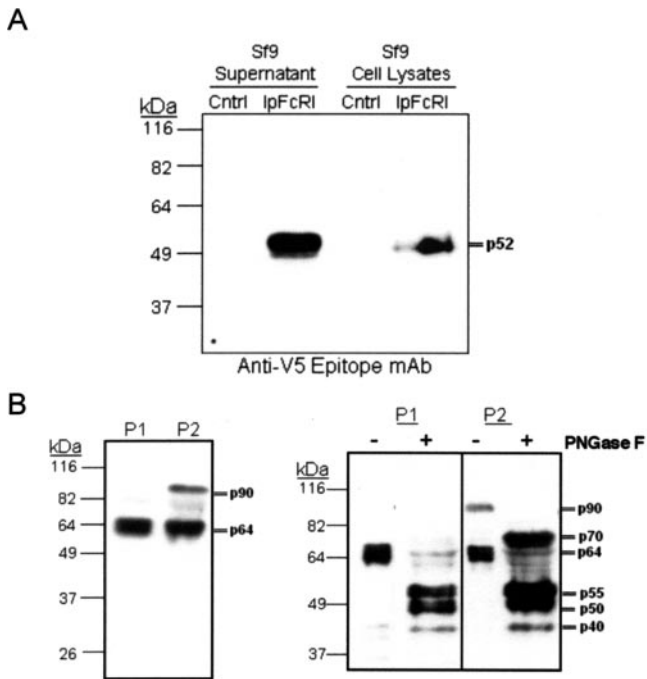
FIGURE 6. Secretion of IpFcRI and detection of the native protein in vivo. *A,* IpFcRI cDNA was cloned into the pIB/V5-His insect expression vector and transiently transfected into Sf9 cells. After 72 h, supernatants (30 μl) and cell lysates (30 μl; ~1 × 10⁶ cells) were examined by Western blot using the anti-V5 epitope mAb. *B,* Detection of native IpFcRI in vivo using a pAb. Plasma samples from two fish (P1 and P2) were separated by reducing SDS-PAGE, transferred to nitrocellulose membranes and then incubated with an anti-IpFcRI pAb (1/3000 (v/v)). Detection of serum IpFcRI was also performed with (+) and without (−) PNGase F treatment before separation by SDS-PAGE.

FIGURE 7. rIpFcRI binds catfish IgM. *A,* Immunoprecipitation of rIpFcRI results in the coimmunoprecipitation of catfish IgM. Two and a half-microliters of precleared CFS was incubated for 14 h at 4°C with 2 μg of refolded rIpFcRI and 1 μg of anti-Xpress mAb or with 1 μg of isotype control mAb (anti-V5) in the presence of 25 μl Sepharose G beads. Washed Sepharose G beads were analyzed by SDS-PAGE and Western blot for the presence of catfish IgM (*left panel*) and rIpFcRI (*right panel*).*B,* Immunoprecipitation of catfish IgM results in the coimmunoprecipitation of rIpFcRI. CFS was incubated with 2 μg of rIpFcRI, 25 μl of Sepharose G beads in the presence of 50 μl mAb 9E1 or 50 μl mAb 1.14 for 14 h at 4°C. Washed Sepharose G beads were analyzed by SDS-PAGE and Western blot for the presence of catfish IgM (*left panel*) and rIpFcRI (*right panel*).

IgM-positive and IgM-negative fractions, it was demonstrated that within PBL, neutrophils appeared to predominantly express IpFcRI. In addition, IgM negative lymphocytes from the anterior and posterior kidney expressed more IpFcRI message than lymphocytes from the peripheral blood. Therefore, the differential expression of IpFcRI in vivo may be in part due to the regionality of the leukocyte subpopulations and/or their activation state. In the absence of available catfish lymphocyte-specific mAbs other than anti-IgM, precise determination of the cells responsible for IpFcRI cannot be accurately determined. However, our expression analysis provides some insights into IpFcRI expression by leukocyte subpopulations in vivo. Several catfish clonal cell lines were also examined, and only the nonautonomous TS32.17 CTL cell line expressed IpFcRI. Following nested PCR, IpFcRI message was also detectable in 3B11 and 1G8 B cells, 42TA macrophages, and a polyclonal MLC, suggesting that the expression levels in vitro are significantly lower than those observed in vivo. At present the factors responsible for regulating IpFcRI expression are unknown. However, increased expression in hemopoietic tissues, freshly isolated leukocyte subpopulations, and enriched PBL-derived neutrophils, suggest that this FcR homolog is widely expressed in vivo.

Coimmunoprecipitation experiments indicated that rIpFcRI produced in *E. coli* recognized native catfish IgM directly in the serum. It also appears that N-linked glycosylation of IpFcRI is not necessary for IgM binding although it is possible that glycosylation could influence affinity. In humans, prokaryotic derived soluble rFcRIIb was generated and refolded using a similar procedure described in this study (65). After refolding, the unglycosylated

rFcRIIb bound to immobilized Ig as well as Ig in solution. Furthermore, mutant mammalian FcR devoid of N-linked glycosylation sites exhibited increased binding to monomeric IgG, compared with the wild-type glycosylated receptors (66). How N-linked glycosylation effects IpFcRI binding properties is presently unknown, but it appears not to be a requirement for the binding observed in this study. IgM binding by IpFcRI also was confirmed using a eukaryotic pDisplay system where transfected HeLa cells expressing surface targeted IpFcRI were shown to bind catfish IgM by FACS analysis. A similar experimental approach using the pDisplay vector has been used to determine whether selected mammalian FCRL (i.e., FREB/FcRX) bind Ig (58). Although FREB/FcRX is similar to IpFcRI in that it does not contain a TM and is related to FcR, it also is quite different. This member of the FCRL lacks any identifiable Fc fragment binding residues, as well as the corresponding D1 Ig-like domain present in the classical FcR sequences and IpFcRI. Because FREB/FcRX does not bind Ig, this further reinforces the notion of the evolutionary importance of the FcR D1D2 Ig domains required for Ab binding.

Amino acid alignments, PDB searches, and protein modeling demonstrated a high degree of structural conservation between IpFcRI and mammalian FcRs, in particular, the D1 and D2 alignments. Eight of the predicted β-strand in the D1 of human FcR are present in similar positions in the corresponding regions of the
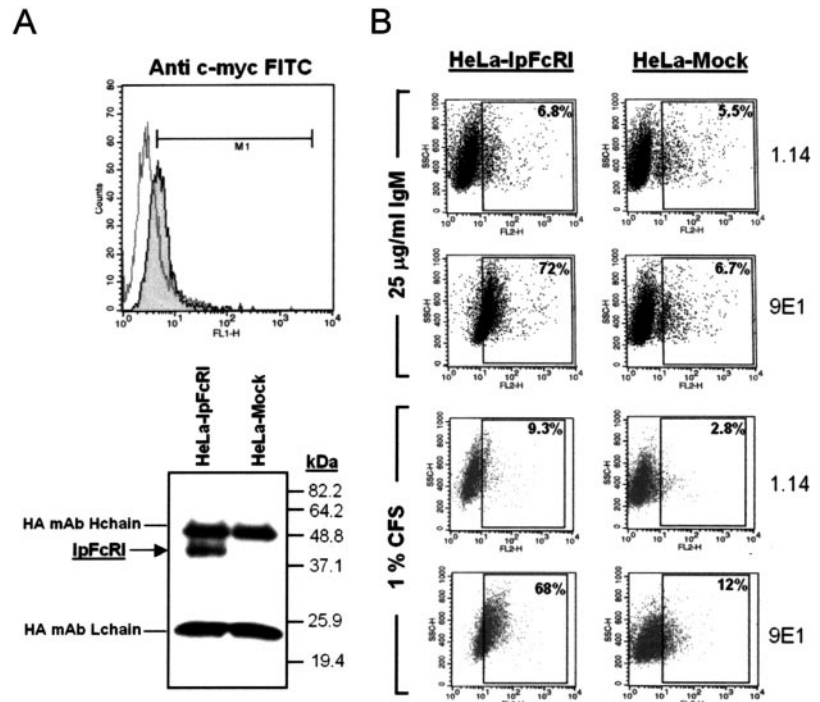
FIGURE 8. Cell surface IpFcRI binds catfish IgM. *A*, Surface expression and increased 9E1 staining of IpFcRI-pDisplay transfected HeLa cells. Mock cells were treated with all transfection reagents without plasmid DNA and cell surface expression by HeLa-IpFcRI was confirmed by flow cytometry using Anti c-*myc* FITC mAb (*upper panel*) and by immunoprecipitation using anti-HA mAb followed by Western blotting with anti-HA mAb (*lower panel*). *B*, Forty eight hours after transfections, both IpFcRI-transfected and mock-transfected HeLa cells were incubated with DMEM supplemented with either 25 µg/ml catfish IgM or 1% CFS for 20 h at 37°C. Surface bound catfish IgM was then detected by staining with the anti-catfish IgM mAb (9E1) and the secondary anti-mouse Ig-biotin conjugated followed by streptavidin-PE (*right panel*). Percentage of gated cells (FL2) stained with 9E1 and with 1.14 (isotype control) are indicated in the top right corner of the individual histograms.

catfish sequence and amino acid identity/similarity among the predicted β-strand was observed. An additional β-strand was predicted in the IpFcRI D1 sequence between the F-G loops of human FcR. Likewise, a similar degree of conservation of β-strand positions and amino acid identity/similarity was observed in the D2 with the exception that the C′ β-strand was not in the IpFcRI sequence. The contention that IpFcRI D1 and D2 were structurally conserved with the corresponding Ig domains of mammalian Ig-binding receptors was further supported by the PDB and SwissProt database searches. The most significant PDB matches were FcR with human FcεRI being identified as the top scoring structural IpFcRI relative with an *E* value of 8e-11. Comparatively, the SwissProt database identified mouse and human FcγRI, FcγRII, FcγRIII, and FcεRI, with *E* values ranging from 4e-7 to 1e-19. Based on this information, an IpFcRI protein model was generated that revealed a folding pattern and overall tertiary structure similar to that of mammalian FcR (61–63). In mammalian FcR, the Ig binding residues are primarily located in the D2 loop regions (62, 63). Specifically, the contact residues are scattered throughout D2 in areas that consist of the B-C, C′-E, F-G loops, and the Cβ strand of the D2 domain. Five of the 15-aa residues known to make contact with the Fc portion of Ig in mammalian FcRs are either identical or conserved within IpFcRI D2. The conservation of all the Fc contact residues is unlikely due to the recognizable variability between mammalian and teleost Ig at both the amino acid and structural levels. However, the structural conservation of the D1D2 Ig-binding domains between mammalian FcRs and the novel IpFcRI does suggest an evolutionary importance of the D1D2 unit for Ig-binding among the vertebrates.

Located among the classical *FcR* on human chromosome 1q21-23 is a family of FcR relatives recently identified by using a consensus FcγR Fc-binding sequence motif to screen the databases (60). These receptors, known as the Fc-related proteins (FCRL), also have been identified in mice (chromosome 3; 67) and, although little is known about their functional roles and specific ligands, their identification has provided insights into the evolution of FcR-like receptors (68). *FCRL* genes appear to be members of

a phylogenetically conserved immune receptor family. Evidence for this notion comes from the recent identification of novel IgSF receptors in ectothermic vertebrates. Of note is the discovery of the *Xenopus* leukocyte FcR-like proteins (XFL; Ref. 64) and the leukocyte immune-type receptors in channel catfish (IpLITR; Ref. 59). These amphibian and teleost molecules represent large and highly diversified families of putative immunoregulatory receptors that are composed of Ig domains related to those of the mammalian FCRL and FcR. Discovery of FCRL, XFL, and IpLITR in combination with detailed phylogenetic analysis of Ig domains encoded by receptors within the mammalian and avian LRC (69) represents the first molecular evidence that FcR-like receptors are present in amphibians and fish. However, the chicken (*Gallus gallus*) is the only nonmammalian species where bona fide Ig-binding FcR homologs have been described (70).

In summary, IpFcRI appears to be a bona fide teleost FcR capable of binding Ig. It is structurally conserved with members of the classical FcRs, and maintains the D1D2 unit and Fc-binding sites required for Ab recognition. Moreover, preliminary functional analysis suggests that IpFcRI binds to catfish Ig as a soluble protein in the serum, or as a receptor when expressed on the cell surface. Although a membrane form of this receptor or other catfish putative Ig-binding molecules have yet to be identified, the discovery of IpFcRI is the first report of an FcR homolog in ectothermic vertebrates. Thus, it represents an important step toward understanding the evolutionary history and functional significance of Ig-binding proteins throughout vertebrates.

Acknowledgments

Disclosures

References

1. Boyden, S. V. 1964. Cytophilic antibody in guinea-pigs with delayed-type hypersensitivity. *Immunology* 7: 474–483.

2. Basten, A., J. F. Miller, J. Sprent, and J. Pye. 1972. A receptor for antibodies on B lymphocytes. *J. Exp. Med.* 135: 610–626.

3. Dickler, H. B. 1974. Studies of the human lymphocyte receptor for heat aggregated of antigen complexed immunoglobulin. *J. Exp. Med.* 140: 508–522.

4. Paraskevas, F., E. D. Anderson, and L. G. Israels. 1972. A feceptor for Fc in mouse B-lymphocytes. *J. Immunol.* 108: 1319–1327.

5. Qui, W. Q., D. de Bruin, B. H. Brownstein, R. Pearse, R., and J. V. Ravetch. 1990. Organization of the human and mouse low-affinity *Fcγ*R genes. *Science* 248: 732–735.

6. Hulett, M. D., and P. M. Hogarth. 1994. Molecular basis for Fc receptor function. *Adv. Immunol.* 57: 1–127.

7. Su, K., J. Wu, J. C. Edberg, S. E. McKenzie, and R. P. Kimberly. 2002. Genomic organization of classical human low-affinity *Fcγ* receptor genes. *Genes Immun.* 3: S51–S56.

8. Osman, N., C. A. Kozak, I. F. C. McKenzie, and P. M. Hogarth. 1992. Structure and mapping of the gene encoding mouse high-affinity *Fcγ*RI and chromosomal location of the human *Fcγ*RI gene. *J. Immunol.* 148: 1570–1575.

9. Nimmerjahn, N., P. Bruhns, K. Horiuchi, and J. V. Ravetch. 2005. FcγRIV: a novel FcR with distinct IgG subclass specificity. *Immunity* 23: 41–51.

10. Metzger, H., G. Alcaraz, R. Hohman, J. P. Kinet, V. Pribluda, and R. Quarto. 1986. The receptor with high affinity for immunoglobulin E. *Annu. Rev. Immunol.* 4: 419–470.

11. Yodoi, J., M. Hosoda, M. Takami, and T. Kawabe. 1989. Regulation of the expression of FcεRII and IgE-BF. *Chem. Immunol.* 47: 106–127.

12. Shibuya, A., N. Sakamoto, Y. Shimizu, K. Shibuya, M. Osawa, T. Hiroyama, H. J., Eyre, G. R. Sutherland, Y. Endo, T. Fujita, et al. 2000. Fcα/μ receptor mediates endocytosis of IgM-coated microbes. *Nat. Immunol.* 1: 441–446.

13. Sakamoto, N., K. Shibuya, Y. Shimizu, K. Yotsumoto, T. Miyabayashi, S. Sakano, T. Tsuji, E. Nakayama, H. Nakauchi, and A. Shibuya. 2001. A novel Fc receptor for IgA and IgM is expressed on both hematopoietic and nonhematopoietic tissues. *Eur. J. Immunol.* 31: 1310–1316.

14. Allen, J. M., and B. Seed. 1989. Isolation and expression of functional high affinity Fc receptor complementary cDNAs. *Science* 243: 378–381.

15. Sears, D. W., N. Osman, B. Tate, I. F. McKenzie, and P. M. Hogarth. 1990. Molecular cloning and expression of the mouse high affinity Fc receptor for IgG. *J. Immunol.* 144: 371–378.

16. Hulett, M. D., and P. M. Hogarth. 1994. Molecular basis for Fc receptor function. *Adv. Immunol.* 57: 1–127.

17. Gavin, A. L., P. S. Tan, and P. M. Hogarth. 1998. Gain-of-function mutations in *Fcγ*RI of NOD mice: implications for the evolution of the Ig superfamily. *EMBO J.* 17: 3850–3857.

18. Toshiyuki, T. 2005. Fc receptors and their role in immune regulation and autoimmunity. *J. Clin. Immunol.* 25: 1–18.

19. Fridman, W. H., J.-L. Teillaud, C. Bouchard, C. Teillaud, A. Astier, E. Tartour, J. Galon, C. Mathiot, and C. Sautes. 1993. Soluble Fcγ receptors. *J. Leukocyte Biol.* 54: 504–512.

20. Ravetch, J. V., and J. P. Kinet. 1991. Fc receptors. *Annu. Rev. Immunol.* 9: 457–492.

21. Astier, A., H. de la Salle, C. de la Salle, T. Bieber, M-E. Esposito-Farese, M. Freund, J-P. Cazenave, W-H. Fridman, J-L. Teillaud, and D. Hanau. 1994. Human epidermal langerhans cells secrete a soluble receptor for IgG (FcγRII/CD32) that inhibits the binding of immune complexes to FcγR+ cells. *J. Immunol.* 152: 201–212.

22. Ravetch, J. V., and B. Perussia. 1989. Alternative membrane forms of FcγRIII(CD16) on human natural killer cells and neutrophils. *J. Exp. Med.* 170: 481–497.

23. Mausda, M., T. Morimoto, S. Kobatake, N. Nishimura, K. Nakamoto, X. H. Dong, Y. Komiyama, R. Ogawa, and H. Takahashi. 2003. Measurement of soluble Fcγ receptor type IIIa derived from macrophages in plasma: increase in patients with rheumatoid arthritis. *Clin. Exp. Immunol.* 132: 477–484.

24. Galon, J., C. Bouchard, W. H. Fridman, and C. Sautes. 1995. Ligands and biological activities of soluble Fcγ receptors. *Immunol. Lett.* 44: 175–181.

25. Galon, J., J.-F. Gauchat, N. Mazieres, R. Spangoli, W. Storkus, M. Lotze, J-Y. Bonnefoy, W.-H. Fridman, and C. Sautes. 1996. Soluble Fcγ receptor type III (FcγRIII. CD16) triggers cell activation through interaction with complement receptors. *J. Immunol.* 157: 1184–1192.

26. Wines, B. D., A. Gavin, M. S. Powell, M. Steinitz, R. R. C. Buchanan, and P. M. Hogarth. 2003. Soluble FcγRIIa inhibits rheumatoid factor binding to immune complexes. *Immunol.* 109: 246–254.

27. Bengtén, E., M. Wilson, N. W. Miller, L. W. Clem, L. Pilstrom, and G.W. Warr. 2000. Immunoglobulin isotypes: structure, function, and genetics. *Curr. Top. Microbio. Immunol.* 248: 189–219.

28. Pure, E., A. D. Luster, and J. C. Unkeless. 1984. Cell surface expression of murine, rat, and human Fc receptors by *Xenopus* oocytes. *J. Exp. Med.* 1: 606–611.

29. Sekizawa, A., T. Fujii, and S. Tochinai. 1984. Membrane receptors on Xenopus macrophages for two classes of immunoglobulins (IgM and IgY) and the third complement component (C3). *J. Immunol.* 133: 1431–1435.

30. Coosemans, V., and I. Hadji-Azimi. 1986. Partial characterization of different cell types found in the *Xenopus laevis* lymphoreticular tumor bases on the presence or absence of surface immunoglobulins and Fc molecules. *Dev. Comp. Immunol.* 10: 547–549.

31. Coosemans, V., and I. Hadji-Azimi. 1988. Immunoglobulin Fc receptor molecules on *Xenopus laevis* splenocytes. *Immunol.* 65: 641–645.

32. Haynes, L., L. Fuller, and E. C. McKinney. 1988. Fc receptors for shark IgM. *Dev. Comp. Immunol.* 12: 561–571.

33. Griffin, B. R. 1983. Opsonic effect of rainbow trout (*Salmo gairdnen*) antibody on phagocytosis of *Yersinia ruckerii* by trout leukocytes. *Dev. Comp. Immunol.* 7: 253–259.

34. Honda, A., H. Kodama, M. Moustafa, F. Yamada, T. Mikami, and H. Izawa. 1986. Phagocytic activity of macrophages of rainbow trout against *Vibrio anguillarum* and the opsonizing effect of antibody and complement. *Res. Vet. Sci.* 40: 328–332.

35. Koumans-van Diepan, J. C. E., M. H. M. Van de Lisdonk, B. M. Taverne-Thiele, L. Verberg van Kemenade, and J. H. W. M. Rombout. 1994. Characterisation of immunoglobulin-binding leukocytes in carp (*Cyprinus carpio L.*). *Dev. Comp. Immunol.* 18: 45–56.

36. O'Dowd, A. M., A. E. Ellis, and C. J. Secombes. 1998. Binding of immune complexes to Atlantic salmon peripheral blood leukocytes. *Dev. Comp. Immunol.* 22: 439–448.

37. Shen, L., T. B. Stuge, J. B. Evenhuis, E. Bengten, M. Wilson, V. G. Chinchar, L. W. Clem, and N. W. Miller. 2003. Channel catfish NK-like cells are armed with IgM via a putative FcμR. *Dev. Comp. Immunol.* 27: 699–714.

38. Bly, J. E., A. S. Grimm, and I. G. Morris. 1986. Transfer of passive immunity from mother to young in a teleost fish: haemagglutinating activity in the serum and eggs of plaice *Pleuronectes platessa L. Comp. Biochem. Physiol. A.* 84: 309–313.

39. Haines, A. N., M. F. Flajnik, L. L. Rumfelt, and J. P. Wourms. 2005. Immunoglobulins in the eggs of the nurse shark *Ginglymostoma cirratum. Dev. Comp. Immunol.* 29: 417–430.

40. van Ginkel, F. W., N. W. Miller, C. J. Lobb, and L. W. Clem. 1992. Characterization of anti-hapten antibodies generated in vitro by channel catfish peripheral blood lymphocytes. *Dev. Comp. Immunol.* 16: 139–151.

41. Miller, N. W., M. A. Rycyzyn, M. R. Wilson, G. W. Warr, J. P. Naftel, and L. W. Clem. 1994. Development and characterization of channel catfish long term B cell lines. *J. Immunol.* 152: 2180–2189.

42. Miller, N. W., V. G. Chinchar, and L. W. Clem. 1994. Development of leukocyte cell lines from the channel catfish (*Ictalurus punctatus*). *J. Tissue Cult. Methods* 16: 117–123.

43. Stuge, T. B., M. R. Wilson, H. Zhou, K. S. Barker, E. Bengten, G. Chinchar, N. W. Miller, and L. W. Clem. 2000. Development and analysis of various clonal alloantigen-dependent cytotoxic cell lines from channel catfish. *J. Immunol.* 164: 2971–2977.

44. Stuge, T. B., S. H. Yoshida, V. G. Chinchar, N. W. Miller, and L. W. Clem. 1997. Cytotoxic activity generated from channel catfish peripheral blood leukocytes in mixed leukocyte cultures. *Cell Immunol.* 177: 154–161.

45. Miller, N. W., J.E. Bly, F. van Ginkel, C. F. Ellsaesser, and L. W. Clem. 1987. Phylogeny of lymphocyte heterogeneity: identification and separation of functionally distinc subpopulations of channel catfish lymphocytes with monoclonal antibodies. *Dev. Comp. Immunol.* 11: 739–747.

46. DeLuca, D., M. Wilson, and G. W. Warr. 1983. Lymphocyte heterogeneity in the trout. *Salmo gairdneri*, defined with monoclonal antibodies to IgM. *Eur. J. Immunol.* 13: 546–551.

47. Altschul, S. F., W. Gish, W. Miller, E. W. Meyers, and D. J. Lipman. 1990. Basic local alignment search tool. *J. Mol. Biol.* 215: 403–410.

48. Quiniou, S. M., T. Katagiri, N. W. Miller, M. Wilson, W. R. Wolters, and G. C. Waldbieser. 2003. Construction and characterization of a BAC library from a gynogenetic channel catfish (*Ictalurus punctatus*). *Genet. Sel. Evol.* 35: 673–683.

49. Thompson, J. D., T. J. Gibson, F. Plewniak, F. Jeanmougin, and D. J. Higgins. 1997. The CLUSTAL_X windows interface: flexible strategies for multiple sequence alignment aided by quality analysis tools. *Nucleic Acids Res.* 24: 4876–4882.

50. Kumar, S., K. Tamura, I. B. Jakobsen, and M. Nei. 2001. MEGA2: molecular evolutionary genetics analysis software. *Bioinformatics* 17: 1244–1245.

51. Letunic, I., R. R. Copley, S. Schmidt, F. D. Ciccarelli, T. Doerks, J. Schultz, C. P. Ponting, and P. Bork. 2004. SMART 4.0: towards genomic data integration. *Nucleic Acids Res.* 32: D142–D144.

52. Bateman, A., L. Coin, R. Durbin, R. D. Finn, V. Hollich, S. Griffiths-Jones, A. Khanna, M. Marshall, S. Moxon, E. L. Sonnhammer, et al. The Pfam protein families database. *Nucleic Acids Res.* 32: D138–D141, 2004.

53. Kelly, L. A., R. M. MacCallum, and M. J. Sternberg. 2000. Enhanced genome annotation using structural profiles in the program 3D-PSSM. *J. Mol. Biol.* 299: 499–520.

54. Miller, S. A., D. D. Dykes, and H. F. Polesky. 1988. A simple salting out procedure for extracting DNA from human nucleated cells. *Nucleic Acids Res.* 16: 1215–1215.

55. Hoelsbrekken, S. E., S. Fossum, and E. Dissen. 2005. Molecular cloning of LILRC1 and LILRC2 in the mouse and the rat, two novel immunoglobulin-like receptors encoded by the leukocyte receptor gene complex. *Immunogenetics* 57: 479–486.

56. van Ginkel, F. W., D. W. Pascual, and L. W. Clem. 1991. Proteolytic fragmentation of channel catfish antibodies. *Dev. Comp. Immunol.* 15: 41–51.

57. Davis, R. S., H. Li, C-C. Chen, Y.-H. Wang, M. D. Cooper, and P. D. Burrows. 2002. Definition of an Fc receptor-related gene (*FcRX*) expressed in human and mouse B cells. *Int. Immunol.* 14: 1075–1083.

58. Facchetti, F., M. Cella, S. Festa, D. H. Fremont, and M. Colonna. 2002. An unusual Fc receptor-related protein expressed in human centoblasts. *Proc. Natl. Acad. Sci. USA* 99: 3776–3781.

59. Stafford J. L., E. Bengten, M. Wilson, L. W. Clem, and N. W. Miller. 2004. Identification and characterization of leukocyte immunoglobulin-like receptors in channel catfish (*Ictalurus punctatus*). *12th Int. Cong. Immunol. and 4th Annu.*

Conf. FOCIS, Montreal, 2004. ⟨www.immuno2004.org/onlineabstracts/categorytoc.html⟩. Abstr. 4090.

60. Davis, R. S., Y. H. Wang, H. Kubagawa, and M. D. Cooper. 2001. Identification of a family of Fc receptor homologs with preferential B cell expression. *Proc. Natl. Acad. Sci. USA* 98: 9772–9777.

61. Sondermann, P., R. Huber, and U. Jacob. 1999. Crystal structure of the soluble form of the human Fcγ-receptor IIb: a new member of the immunoglobulin superfamily at 1.7 A resolution. *EMBO J.* 18: 1095–1103.

62. Garman, S. C., B. A. Wurzburg, S. S. Tarchevskaya, J-P. Kinet, and T. S. Jardetzky. 2000. Structure of the Fc fragment of human IgE bound to its high-affinity receptor FcεRIα. *Nature* 406: 259–266.

63. Radaev, S., S. Motyka, W-H. Fridman, C. Sautes-Fridman, and P. S. Sun. 2001. The structure of a human type III Fcγ receptor in complex with Fc. *J. Biol. Chem.* 276: 16469–16477.

64. Guselnikov, S. V., A. Erilova, A. M. Najakshin, N. Cohen, J. Robert, and A. V. Taranin. 2004. FcR-like genes in the amphibian *Xenopus*: species-specific expansion, structural diversity, and developmental expression. *12th Int. Cong.*

Immunol. and *4th Annu. Conf. FOCIS*, Montreal, 2004. ⟨www.immuno2004.org/onlineabstracts/ categorytoc.html⟩. Abstr. 2881.

65. Sondermann, P., and U. Jacob. 1999. Human Fcγ receptor IIb expressed in *Escherichia coli* reveals IgG binding capability. *Biol Chem.* 380: 717–721.

66. Drescher, B., T. Witte, and R. E. Schmidt. 2003. Glycosylation of FcγRIII in N163 as a mechanism of regulating receptor affinity. *Immunology* 110: 335–340.

67. Davis, R. S., R. P. Stephan, C. C. Chen, G. Dennis, Jr., and M. D. Cooper. 2004. Differential expression of mouse Fc receptor homologs. *Int. Immunol.* 16: 1343–1353.

68. Davis, R. S., G. R. A. Ehrhardt, C. M. Leu, M. Hirano, and M. D. Cooper. 2005. An extended family of Fc receptor relatives. *Eur. J. Immunol.* 35: 674–680.

69. Nikolaidis, N., J. Klein, and M. Nei. 2005. Origin and evolution of the Ig-like domains present in mammalian leukocyte receptors: insights from chicken, frog, and fish homologues. *Immunogenetics* 57: 151–157.

70. Manghi, M. A., S. M. Venturiello, M. I. Guterrez, M. Etchevierrigaray, and R. A. Margni. 1987. Isolation and partial characterization of biologically active Fc receptor of chicken red cells. *Biochim. Biophys. Acta* 923: 381–388.